New BIOTECHNOLOGY 90 (2025) 88–96

Contents lists available at ScienceDirect

New BIOTECHNOLOGY

journal homepage: www.elsevier.com/locate/nbt

Prenylation of diverse indole derivatives by the fungal aromatic prenyltransferase RePT

Pimvisuth Chunkrua, Mirjam A. Kabel, Jean-Paul Vincken, Willem J.H. van Berkel, Wouter J.C. de Bruijn *

Laboratory of Food Chemistry, Wageningen University, Bornse Weilanden 9, Wageningen 6708 WG, the Netherlands

ARTICLE INFO

Keywords:
Biocatalysis
Fungal
Halogen
Indole
Prenylation
Synthase
Bioactive natural products
Antimicrobial

ABSTRACT

Prenylation is a widespread natural modification of compounds that serves to functionalize and often enhance the bioactivity of plant and microbial secondary metabolites, including indole derivatives. In this study, we aimed to expand the library of prenylated indoles using RePT, a fungal (i.e. *Rasamsonia emersonii*) aromatic prenyltransferase from the dimethylallyl tryptophan synthase (DMATS) family. Previous work showed that RePT readily *C*7- and *N*1-prenylated L-tryptophan, and *O*-prenylated L-tyrosine and a number of phenolic stilbenes. Here, we investigated its regioselectivity further with 23 indole substrates, including tryptophan derivatives with varying *C*4-*C*7 substituents and several *C*3-substituted indoles. High conversion was observed primarily with fluorinated tryptophans and unsubstituted indole. Product analysis by UHPLC-PDA-ESI-MS^n and NMR revealed that RePT mainly catalyzed either normal prenylation at *C*7 or reverse prenylation at *N*1 on a series of halogenated tryptophans. The regioselectivity observed for several substrates was strongly influenced by the position of the halogen substituent, particularly fluorine, which displayed its characteristic *ortho-/para*-directing effect. In the absence of the amino acid moiety, RePT's regioselectivity in some cases shifted from its typical preference, leading to prenylation at alternative positions such as *C*3 and *C*6. These findings showcase the versatility of RePT for modifying diverse indole derivatives and demonstrate, for the first time, halogen-induced steering of the regioselectivity of DMATS to facilitate synthesis of bioactive prenylated compounds and intermediates.

1. Introduction

Indole alkaloids comprise a large group of natural products present in terrestrial and marine microbes and plants [1]. Many of these alkaloids, particularly those from fungi, are known for their therapeutic properties and are therefore used in various pharmaceuticals [2–8] (Fig. 1). Biologically active indole alkaloids often derive from prenylated L-tryptophan or its derivatives [1] (Fig. 1). Prenylation refers to the attachment of an isoprenoid unit, such as a prenyl or geranyl moiety. In biosynthesis, the prenylated intermediate subsequently proceeds through a series of steps [9], resulting in an indole alkaloid that either retains the intact prenyl group or integrates it into a new skeleton. The prenyl group is not only a key structural feature of the exemplified biologically active indole alkaloids, but prenylation has also been shown to generally enhance antimicrobial activity of natural products [10,11], likely by increasing their hydrophobicity and thereby their affinity for biological membranes [12,13]. Given that indoles form the core scaffold of many biologically active compounds, and that prenylation can enhance their activity or provide a functional group for further modifications to obtain valuable chemicals [9], the synthesis of structurally diverse prenylated indoles is of growing interest [14].

In nature, dimethylallyl tryptophan synthases (DMATSs) are the enzymes that catalyze the regioselective aromatic prenylation in fungal and bacterial indole alkaloid biosynthesis routes [15]. In general, DMATSs transfer an isoprenoid moiety from a prenyl donor substrate, such as C5- (dimethylallyl), C10- (geranyl), or C15- (farnesyl) pyrophosphate, to an aromatic acceptor substrate. The enzymatic prenylation can occur in either a normal configuration, which is attachment of the prenyl group via its *C*1, or a reverse configuration, which is attachment via its *C*3. Most characterized DMATSs have been shown to utilize dimethylallyl pyrophosphate (DMAPP) to perform prenylation of tryptophan or tyrosine derivatives [16–20].

Many of the currently known biologically active indole alkaloids derive from *C*2- or *C*4-prenylated tryptophan (Fig. 1). Examples of

* Corresponding author.
E-mail address: wouter.debruijn@wur.nl (W.J.C. de Bruijn).

https://doi.org/10.1016/j.nbt.2025.09.002
Received 12 June 2025; Received in revised form 9 August 2025; Accepted 8 September 2025
Available online 16 September 2025

medicinal drugs produced from prenylated tryptophan intermediates include the semisynthetic ergot alkaloids bromocriptine and methylergonovine, which share D-lysergic acid derived from *C*4-prenyl-L-tryptophan as their precursor [21,22]. Other examples are tryprostatins, which involve intermediate normal *C*2-prenylation of the cyclic dipeptide brevianamide F (cyclo(L-Trp-L-Pro)) [23]. Furthermore, reverse *C*2-prenylation of cyclo(L-Trp-L-Pro) followed by a series of modifications, including *C*7-prenylation, leads to the biosynthesis of (−)-notoamide A [24].

Driven by the pharmaceutical potential of these prenylated molecules, we aimed to expand the library of prenylated indole derivatives using a recently discovered fungal DMATS from *Rasamsonia emersonii*, named RePT [25]. It has been shown that RePT readily *O*-prenylates a number of phenolic stilbenes and L-tyrosine, and that this enzyme is able to prenylate L-tryptophan at the *C*7- and *N*1-position [25]. However, the ability of RePT to catalyze prenylation of other indole derivatives has

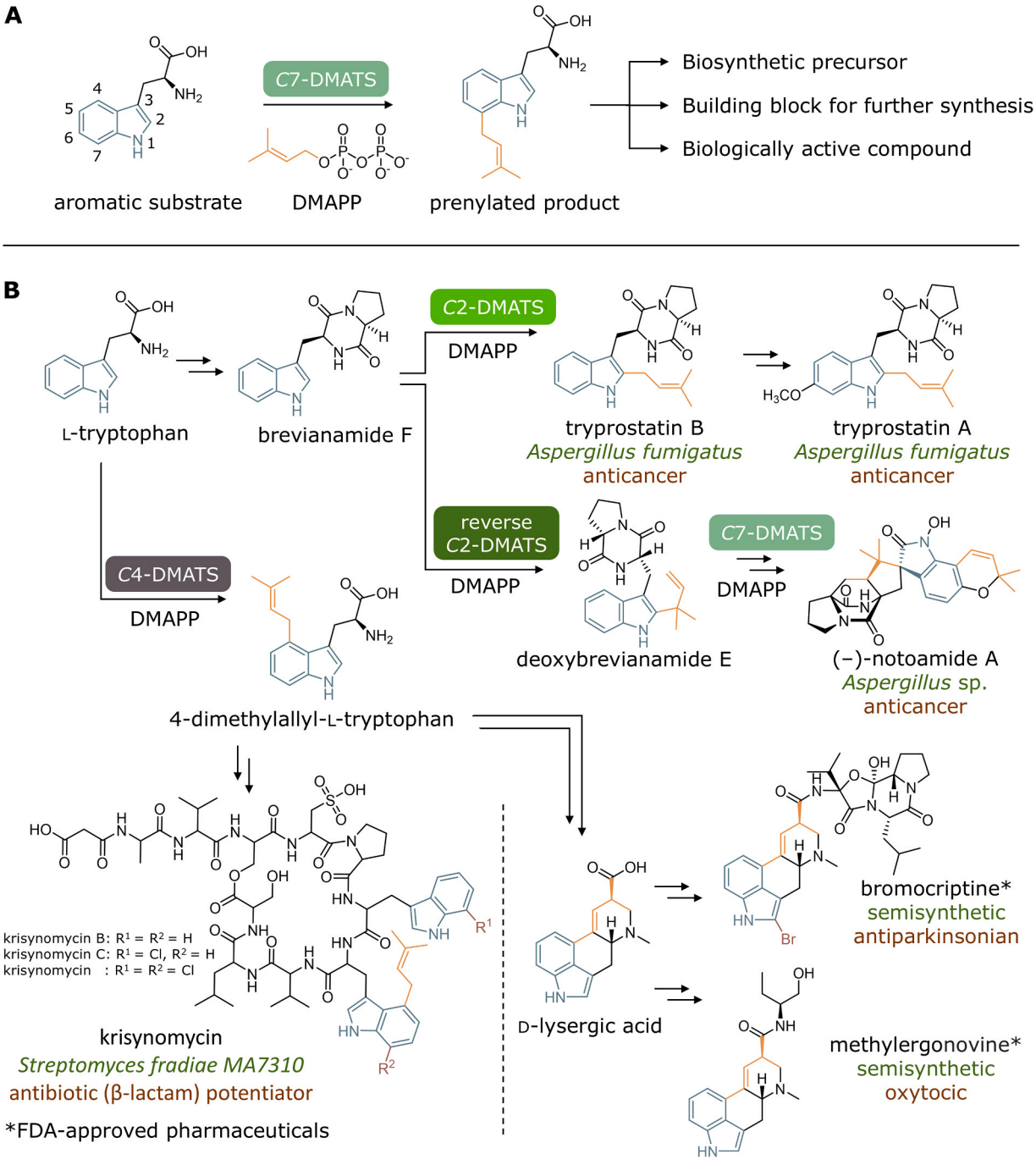

Fig. 1. Prenylation of indole derivatives by DMATSs. A) Example of a regioselective prenylation reaction and potential applications of the prenylated product. Prenylation of indole derivatives can be catalyzed by DMATSs, which is illustrated here with the *C*7-prenylation of L-tryptophan (acceptor substrate) with DMAPP (donor substrate) by a 7-DMATS. Prenylated indole derivatives serve as precursors or intermediates for the formation of several biologically active indole alkaloids. B) Simplified bio- or semisynthetic pathways of bioactive compounds involving DMATS-catalyzed prenylation at various positions on the indole moiety. The scheme illustrates that DMATSs can catalyze either normal prenylation via attachment at *C*1 of the prenyl (e.g. tryprostatin B) or reverse prenylation via attachment at *C*3 of the prenyl (e.g. deoxybrevianamide E). Steps indicated with two arrows involve multiple reactions involving additional (bio)catalysts, which are not detailed here. The indole, prenyl, and halogen moieties are shown in blue, orange, and burgundy, respectively.

not yet been studied. Therefore, this research aimed to explore the prenylation of structurally diverse indole derivatives by RePT and to characterize the resulting products. We focused mainly on the ability of RePT to catalyze prenylation of halogenated tryptophans, as halogenation is commonly found to enhance the pharmaceutical properties of molecules and is used to introduce reactive groups for subsequent reactions in intermediate synthesis steps [26,27]. For example, chlorination of the prenylated indole moiety in krisynomycin significantly enhances its antibacterial and antibiotic potentiating activities compared to its less chlorinated counterparts, krisynomycin B and C [8]. As only a few DMATSs have been reported to accept halogenated tryptophans [16,28], we particularly addressed the potential of RePT to expand the range of prenylated halogenated tryptophans. DMATSs catalyze prenylation by means of electrophilic substitution [22] and halogen substituents will alter the electronic distribution across the indole moiety. Therefore, it is expected that halogenation of the substrates will influence RePT's activity and its product profile.

Furthermore, specifically *C*3-substituted indole derivatives have been indicated as potentiator of multiple antibiotics. For example, camalexin, a secondary metabolite from Brassicaceae plants, has been recently found to act as a potentiator of multiple antibiotics by inhibiting the AcrB efflux pump in *Escherichia coli* [29]. Therefore, we also investigated the ability of RePT to prenylate a series of (biologically active) *C*3-substituted indole derivatives to further expand the library of potentially bioactive indole derivatives.

2. Materials and methods

2.1. Materials

Aromatic compounds tested in the substrate screening for RePT were obtained from suppliers as listed in Table S1. The DMAPP-ammonium salt used for biochemical characterization of RePT was purchased from Sigma-Aldrich (St. Louis, MO, USA), while DMAPP-triammonium salt used for the scaled-up production of prenylated products was synthesized according to the method described in Chunkrua et al. (2024) [25]. Other chemicals were purchased from Sigma-Aldrich and Fisher Scientific (Landsmeer, The Netherlands). UHPLC-MS grade solvents used in UHPLC-PDA-ESI-MS^n analyses were purchased from Biosolve (Valkenswaard, The Netherlands). Water used for purposes other than UHPLC-PDA-ESI-MS^n was purified using a Merck Millipore Milli-Q water purification system (Billerica, MA, USA).

2.2. Gene expression and enzyme purification

Expression and purification of RePT (NCBI accession number: XP_013322739.1), tagged with an N-terminal His-tag linked to a SUMO protein, was performed as previously described [25]. Briefly, the pBAD vector encoding His_6-SUMO-RePT was transformed into *E. coli* NEB 10-beta cells (New England Biolabs, Ipswich, MA). A preculture of 8 mL containing lysogeny broth with ampicillin (0.05 mg/mL) was incubated (37 °C, 16 h, 200 rpm) and later transferred into a 800 mL culture containing Terrific broth and ampicillin (0.05 mg/mL) for further incubation (37 °C, 200 rpm) until the OD_{600} reached 0.6–0.8. Overexpression of the *RePT* gene was induced with L-arabinose (0.2 mg/mL), after which the culture was incubated for another 40 h (24 °C, 200 rpm). Cells were harvested, lysed by sonication, and the cell-free extract was loaded onto a 5 mL HisTrap FF column (Cytiva, Uppsala, Sweden), equilibrated in starting buffer (50 mM Tris/HCl buffer pH 7.5 containing 500 mM NaCl, 10 % (*w/v*) glycerol, and 25 mM imidazole), and connected to an ÄKTA Pure M150 system (Marlborough, MA, USA). After washing the column with the starting buffer until no absorbance at 280 nm was detected, the RePT protein was eluted with a gradient of 25–500 mM imidazole in starting buffer. Purified protein fractions were pooled, desalted, and concentrated using ultra-centrifugal filters with 30 kDa molecular weight cut-off (Merck Millipore, Billerica, MA, USA) and with multiple rounds of centrifugation (4 °C, 4,000 × *g*, 15 min per round). The purified protein was stored in 50 mM Tris/HCl buffer (pH 7.5) containing 10 % (*w/v*) glycerol at -20 °C.

2.3. Substrate screening of RePT

For substrate scope determination, the enzymatic reactions were conducted in 100 µL mixtures of 50 mM Tris/HCl buffer (pH 7.5) with final concentrations of 0.4 mM aromatic acceptor, 0.8 mM prenyl donor, and 100 µg (15 µM) RePT. Two types of controls were included: controls containing the substrate that were subjected to incubation conditions in absence of DMAPP and RePT, which were used as references to determine substrate conversion; and controls containing the substrate that were not subjected to incubation, which were used as references to determine substrate recovery. To standardize the semi-quantification of substrates and products, 3,4,5-trimethoxycinnamic acid (Tokyo Chemical Industry Europe, Zwijndrecht, Belgium) was used as an internal standard at a final concentration of 0.16 mM. Reaction mixtures contained up to 4 % (*v/v*) methanol or DMSO, or 0.4 mM NaOH, depending on the solvent used to dissolve the substrate. All samples and controls were prepared in duplicate and incubated at 37 °C with stirring at 700 rpm for 24 h. The reactions were stopped by adding 200 µL of methanol, followed by centrifugation (4 °C, 18,000 × *g*, 10 min). The supernatants were collected and stored at 4 °C for further analysis using UHPLC-PDA-ESI-MS^n.

2.4. Substrate conversion and product profile analysis by UHPLC-PDA-ESI-MS^n

Substrates and their prenylated derivatives were analyzed using a Thermo Vanquish UHPLC system (Thermo Scientific, San Jose, CA, USA) equipped with a PDA detector. The supernatants obtained after enzyme incubation (1 µL) were loaded onto an Acquity UPLC BEH C18 column (150 mm × 2.1 mm, 1.7 µm) with a VanGuard pre-column of the same material (5 mm × 2.1 mm, 1.7 µm) (Waters, Milford, MA, USA). The column temperature was set at 45 °C, with post-column cooling to 40 °C. The PDA detector recorded the absorbance from 200 to 600 nm. The flow rate was set at 400 µL/min with the following eluents: (A) water with 0.1 % (*v/v*) formic acid and (B) acetonitrile with 0.1 % (*v/v*) formic acid. The elution profile was programmed as follows: 1 min isocratic at 1 %B; 28 min linear gradient from 1 % to 80 %B; 1 min linear gradient from 80 % to 100 %B; 5.5 min isocratic 100 %B; 1 min linear gradient from 100 % to 1 %B; and 5.5 min isocratic at 1 %B.

Mass spectrometric analysis was performed by in-line coupling of the Thermo Vanquish UHPLC system to an LTQ Velos Pro ion trap mass spectrometer (IT-MS) (Thermo Scientific, San Jose, CA, USA) equipped with a heated electrospray ionization (ESI) probe. Nitrogen served as sheath gas (50 arbitrary units), auxiliary gas (13 arbitrary units), and sweep gas (1 arbitrary units). The ion transfer tube was maintained at 263 °C, with a source heater temperature of 425 °C, and source voltages of 2.5 kV for negative ionization (NI) and 3.5 kV for positive ionization (PI) mode. Full scan MS data were acquired in both PI and NI modes, covering an *m/z* range with a lower limit depending on the molecular mass of the substrate and an upper limit of 1,000. MS^2 spectra of all compounds were obtained using data-dependent collision-induced dissociation (CID) fragmentation of the most abundant MS^1 ion with a normalized collision energy of 35 %. Dynamic mass exclusion was used to acquire MS^2 spectra of less intense ions present in MS^1. The most intense ion was fragmented three times with a repeat duration of 5 s and then excluded from fragmentation for 5 s. Data processing was performed using Xcalibur (version 4.4, Thermo Scientific).

Substrate recovery (%) and substrate conversion (%) were calculated based on peak area at $UV_{280\ nm}$, except for compound 26, for which the peak area at $UV_{258\ nm}$ was used. Substrate recovery was determined to indicate stability of the substrates throughout the incubation. Calculations were performed using the following equations:

$$substrate\ recovery(\%) = \frac{Area_{ctrl_0} - Area_{ctrl}}{Area_{ctrl_0}} \times 100 \quad (1)$$

$$substrate\ conversion(\%) = \frac{Area_{ctrl} - Area_r}{Area_{ctrl}} \times 100 \quad (2)$$

The abbreviations are defined as follows: $Area_{ctrl_0}$ = peak area of the substrate in the control sample (without RePT and prenyl donor) without incubation; $Area_{ctrl}$ = peak area of the substrate in the control sample incubated under the same conditions as the reaction mixture; $Area_r$ = peak area of the substrate in the reaction mixture. Substrate recovery data is shown in Table S2.

2.5. Upscaled production of prenylated products

To achieve higher product yields for characterization of the products by NMR spectroscopy, four different reaction conditions were tested with selected substrates (i.e., 7, 8, 9, 10, 16, 17, and 23; Table S1). Each 100 µL reaction mixture contained 50 mM Tris/HCl (pH 7.5), 1 mM aromatic substrate, 1.5 mM DMAPP, RePT at either 0.1 or 1.0 mg/mL, and $CaCl_2$ at either 0 or 5 mM. Samples were incubated at 37 °C for 24 h. Based on the preliminary results of the varying conditions (Fig. S8-9), the enzyme concentration for each substrate was adjusted in expectation of reaching a complete substrate conversion while minimizing enzyme usage (Table S5), and a calcium chloride concentration of 5 mM was applied.

To obtain approximately 4 mg of the main prenylated products for each selected substrate, the reactions were conducted in 17–20 mL (for substrates 7, 8, 9, 10, 16, 17) or 60 mL (for 23) of 50 mM Tris/HCl buffer (pH 7.5) containing 5 mM $CaCl_2$, 1 mM substrate, 1.8 mM DMAPP, and 0.2–0.3 mg/mL RePT. The mixtures were incubated at 37 °C for up to 28 h in an oven without agitation. After incubation, mixtures were centrifuged (4 °C, 4,500 × *g*, 15 min), and the supernatants were separated. The remaining pellets were then extracted three times (3 mL each). The first and second extractions were performed using acetonitrile containing 0.1 % (*v/v*) formic acid at a concentration close to the concentration which eluted the prenylated products in the UHPLC separation, while the third extraction used a higher percentage of acetonitrile (Table S5). The three extracts were combined and the enzymatic products were purified using solid-phase extraction (SPE) with Sep-Pak C18 6 cc Vac cartridges containing 500 mg sorbent (Waters, Milford, MA, USA) attached to an SPE vacuum manifold system (Waters, Milford, MA, USA). The columns were conditioned with 2 × 5 mL of acetonitrile and equilibrated with 5 × 5 mL of 0.1 % (*v/v*) formic acid in the concentration of acetonitrile as used in the starting condition for each substrate. Before sample loading, the acetonitrile concentration of the extracts was adjusted to match the concentration used for column equilibration. Samples were loaded onto the column and elution was performed with stepwise increases in the concentration of acetonitrile containing 0.1 % (*v/v*) formic acid (8 mL each). Fractions were analyzed with UHPLC-PDA-ESI-MS^n to confirm the presence of the prenylated products. Fractions containing the compound(s) of interest were pooled, dried under a nitrogen stream at 35 °C overnight, lyophilized, and stored at -20 °C for further analysis. For details on the reaction conditions, and the extraction and purification steps for each substrate, see Table S5.

2.6. Structure elucidation of prenylated products with NMR spectroscopy

Purified prenylated product (approximately 1.5 mg) was dissolved in 600 µL of methanol-d_4 (Sigma-Aldrich, St. Louis, MO, USA) or DMSO-d_6 (Eurisotop, Saint-Aubin, France). NMR spectra were recorded on a Bruker Avance III UltraShield Plus 600 spectrometer with a cryoprobe or a Bruker Avance III HD Ascend 700 spectrometer with a BBI probe (Bruker, Billerica, MA, USA) at MAGNEFY (MAGNEtic resonance research FacilitY, Wageningen, The Netherlands). The probe temperature was set to 300 K. Data acquisition included one-dimensional ^1H and ^{13}C, and two-dimensional heteronuclear multiple bond correlation (HMBC) and heteronuclear quantum coherence (HSQC) NMR spectra, with additional homonuclear correlation spectroscopy (COSY) spectra for 17d, 17e, 23a, 23c and 23d. Data processing was performed using TopSpin (version 4.1.4, Bruker).

2.7. Accurate mass analysis by UHPLC-ESI-Orbitrap-MS

Purified prenylated compounds were dissolved and diluted in methanol to a final concentration of approximately 20 µg/mL and analyzed using a Thermo Vanquish UHPLC system (Thermo Scientific, San Jose, CA, USA). The sample (1 µL) was loaded onto an Acquity UPLC BEH C18 column (150 mm × 2.1 mm, 1.7 µm) with a VanGuard pre-column (5 mm × 2.1 mm, 1.7 µm) (Waters, Milford, MA, USA). The column temperature was set at 45 °C. The flow rate was set at 400 µL/min with the following eluents: (A) water with 0.1 % (*v/v*) formic acid and (B) acetonitrile with 0.1 % (*v/v*) formic acid. The elution profile was programmed as follows: 1.1 min isocratic at 0 %B; 36.6 min linear gradient from 0 % to 100 %B; 5.5 min isocratic at 100 %B; 1.1 min linear gradient from 100 % to 0 %B 5.5 min isocratic 100 %B; 1 min linear gradient from 100 % to 0 %B; and 5.5 min isocratic at 0 %B.

Accurate mass spectra were recorded by in-line coupling of the Thermo Vanquish UHPLC system to an Orbitrap IQ-X Tribrid mass spectrometer (Thermo Fisher Scientific, San Jose, CA, USA). Prior to analysis, the Orbitrap mass spectrometer was calibrated via the automatic internal calibration function using a Pierce FlexMix Calibration Solution for Auto Ready Mass Spectrometers (Thermo Scientific). Nitrogen served as a sheath gas (50 arbitrary units), auxiliary gas (10 arbitrary units), and sweep gas (1 arbitrary unit). Heated Electrospray Ionization (HESI) was maintained at 325 °C, with a source temperature of 225 °C, and source voltages of 2.5 kV for negative ionization and 3.5 kV in positive ionization mode. Spectra were measured at 120,000 FWHM mass resolution in the *m/z* range of 150–1,000. To provide stable accurate mass data during the analytical runs, fluoranthene was measured continuously as an internal calibrant. All spectra were acquired in profile mode. The absolute AGC target level was set at 1×10^5, the maximum injection time at 1,000 ms, the microscans at 1, and the RF lens at 60 %. Data processing was performed using Xcalibur 4.5 and Freestyle 1.8 (Thermo Scientific).

3. Results and Discussion

3.1. Characterization of prenylated products

To evaluate the ability of RePT to prenylate indole derivatives and to better understand the effect of substituents on regioselectivity of prenylation by RePT, we screened the conversion and product profile with 23 substrates (Table S1 and Fig. S1), which included L-tryptophan (1) with various substituents on *C*4, *C*5, *C*6, and *C*7 of the benzene moiety (3-15), and indole (23) with different substituents on *C*3 of the pyrrole moiety (16-23).

The identification of prenylated products and our strategy used for the (tentative) identification of the prenylation type (*C*-, *O*-, or *N*-prenylation) is explained in detail in Method S1. Tentative identification of most compounds was performed using the UHPLC-PDA-ESI-MS^n data (Table S3), primarily based on their ESI-MS^2 spectra and a decision guideline established in this work (Fig. S2). A group of prenylated compounds was selected for upscaling to mg-scale, allowing structural elucidation via NMR analysis (Fig. 2 and Table S6): prenylated fluoro-L-tryptophans (7a, 7b, 8a, 9b), prenylated indole-3-acetic acids (17d, 17e), prenylated indole-3-propionic acid (18c), and (di)prenylated indoles (23a, 23c, 23d). Structure elucidation was performed with ^1H NMR, ^{13}C NMR, HMBC, and HSQC. COSY was included for compounds 17d, 17e, 23a, 23c, 23d. Although the product fractions after purification in most cases contained more than one product, the chemical structure of the

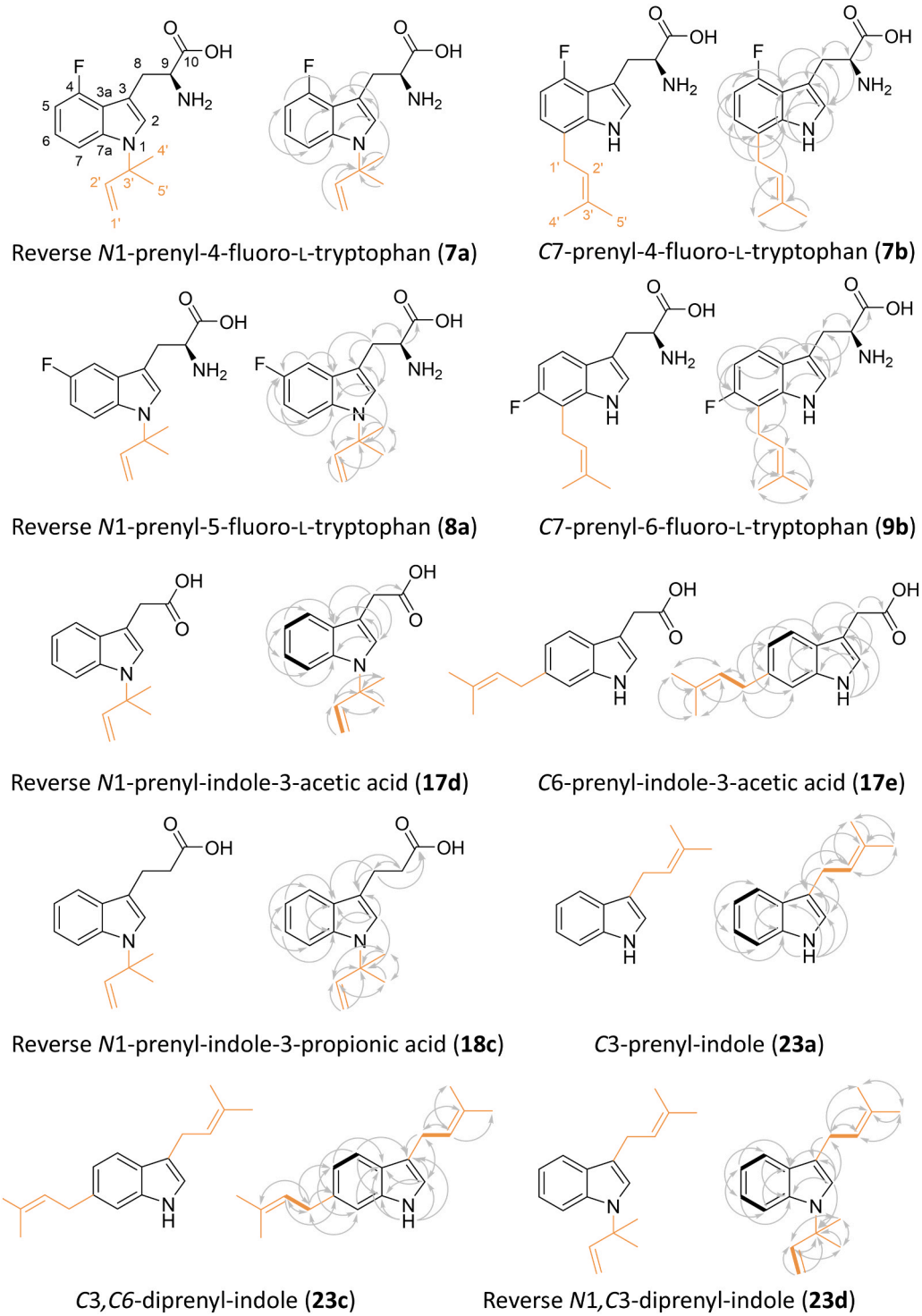

Fig. 2. Chemical structures of prenylated products elucidated using NMR. The prenyl moieties are highlighted in orange. The arrows indicate HMBC correlations. For compounds 17d, 17e, 23a, 23c, and 23d, the bonds displayed in bold indicate COSY correlations.

main products could be reliably identified. The assigned chemical shifts of the products are shown in Table S6. All HMBC correlations can be found in Fig. 2. It is worth noting that the proportion (relative abundance) of each prenylated product as observed in UHPLC-PDA (Table S3) was close to the ratio of the signal intensity between the products in the NMR spectra. Therefore, the elucidated structure could be linked to the assigned peak in the UHPLC-PDA-ESI-MS^n analysis. A more detailed description of the interpretation of NMR spectral data can be found in Appendix D.

The exact mass of above described purified products, as measured by UHPLC-ESI-Orbitrap-MS, and their molecular formulae are shown in Table S7. The prenylation type of all purified compounds that were characterized with NMR was identical to the tentative identification using our decision guideline (Fig. S2), validating the applicability of our UHPLC-PDA-ESI-MS^n tentative identification strategy.

3.2. General observations about the conversion of indole derivatives by RePT

Most DMATSs accept tryptophan for prenylation, and a clear preference for the L-configuration of this aromatic amino acid has been established [16,30–32]. Only in rare occasions the D-enantiomer of tryptophan derivatives is more preferred [33]. In our previous study, RePT was already shown to prenylate L-tryptophan [25]. Here, we tested the ability of RePT to prenylate D-tryptophan. As expected, L-tryptophan (1) was strongly preferred (100 % conversion) by RePT over its D-enantiomer (2) (20.8 % conversion) (Fig. S4). Therefore, all further experiments were performed with the L-enantiomers of the various tryptophan derivatives.

In general, RePT was flexible in accepting *C*4-*C*7 substituted L-tryptophans (3-15, Table S1), showing the highest conversion for fluorinated derivatives (>75 %; Fig. 3). Methylation at *N*1 of the indole moiety of L-tryptophan resulted in near complete loss of conversion. Replacing the aliphatic backbone of tryptophan at *C*3 with different moieties (16-23, Table S1) affected the conversion differently, but mostly reduced the conversion to less than 50 % (Fig. 4).

The conversion of indole derivatives by RePT tended to yield at least two mono-prenylated products (Figs. 3–4). For unsubstituted indole (23), di-prenylated products were also found (Fig. S1, Table S6). Beyond these generic observations, below we discuss in detail the effect of different substituents on the prenylation efficiency, type of prenylation, and regioselectivity of RePT.

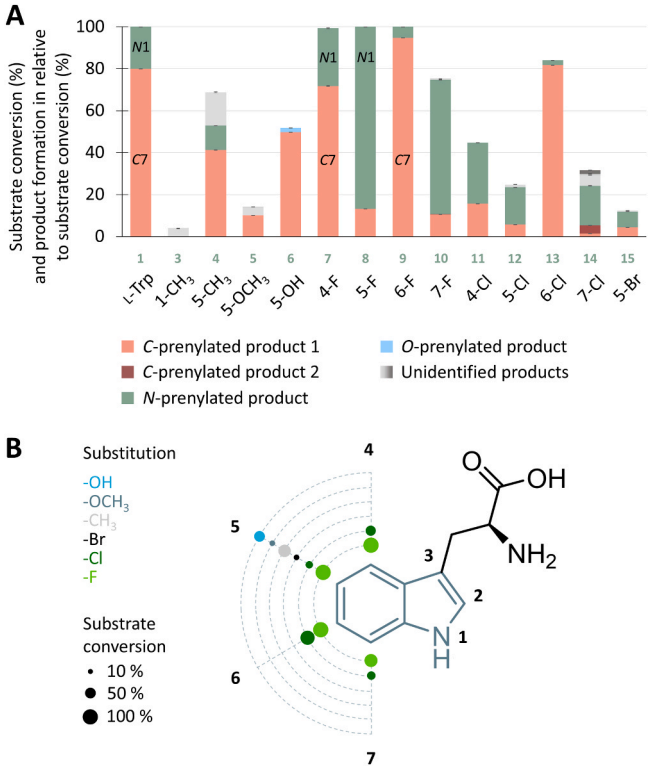

Fig. 3. Prenylation of tryptophan derivatives with varying substituents by RePT in the presence of DMAPP. A) Substrate conversion and product profile. Selected prenylated products whose chemical structures were confirmed by NMR analysis are labeled with their prenylation site (normal *C*7- or reverse *N*1-prenylation). The standard deviations indicated are the deviations for each product's formation relative to substrate conversion (%), while the standard deviations for substrate conversion are provided in Table S3. B) Visualization of the substrate conversion from A), highlighting the influence of both the substituents' type and their position on the conversion.

3.3. Effect of N1-methylation of tryptophan on prenylation by RePT

Because of the *N*1-prenylating ability of RePT towards L-tryptophan [25], it was tested whether RePT could still accept *N*1-methylated L-tryptophan (3). Hardly any prenylation (< 4.0 %) of compound 3 by RePT was observed (Fig. 3). The NH on the pyrrole ring is known to play a crucial role in the prenylation mechanism in DMATSs by forming a hydrogen bond with the carboxyl group of the strictly conserved glutamate in the active site of DMATSs (Fig. S6) [22]. This interaction consequently increases the reactivity of the indole ring to facilitate the prenylation, contributes partially to substrate-binding, and helps stabilize the arenium intermediate [34]. Furthermore, in the case of $DMATS1_{Ff}$, an *N*1-DMATS, the glutamate performs the final deprotonation step to yield the *N*1-prenylated product [35]. The *N*1-methylation therefore likely hindered the ability of the enzyme to interact with the indole ring, thus decreasing the substrate's reactivity and at the same time preventing *N*1-prenylation. Poor conversion of 3 was also reported for various other DMATSs such as FgaPT2 (a 4-DMATS) [16] and $7\text{-}DMATS_{Neo}$ [18], but others such as $5\text{-}DMATS_{Ac}$ [19] and IptA (a bacterial 6-DMATS) [17] converted 3 comparable to or even better than *C*-methylated-DL-tryptophans.

3.4. Effect of various C5-substituents of L-tryptophan on (regioselective) prenylation by RePT

To gain initial insight into how different substituents affect substrate conversion and product profile of RePT, we performed enzymatic reactions with L-tryptophan (1) and L-tryptophans possessing different substituents at the *C*5-position on the benzene ring (Table S1): methyl (4), methoxy (5), hydroxy (6), fluorine (8), chlorine (12), and bromine (15). Like 1, 5-fluoro-L-tryptophan (8) was completely converted (100 ± 0.0 %) under the conditions applied. The order of extent of conversion of the other *C*5-substituted L-tryptophans was: methyl- (68.8 ± 0.3 %), hydroxy- (51.8 ± 0.1 %), chloro- (24.8 ± 0.3 %), methoxy- (14.2 ± 2.0 %), and bromo-L-tryptophan (12.4 ± 0.2 %) (Fig. 3). The fact that the fluorine substituent had the least impact on substrate conversion by RePT is interesting, considering that halogens have a strong inductively electron-withdrawing nature relative to hydrogen [36], and would be expected to have a deactivating effect on DMATS-catalyzed electrophilic aromatic substitution, as reported for another DMATS [37]. We speculate that in our case, the mesomeric electron-donating character of fluorine [38] may facilitate the prenylation by increasing the nucleophilicity of the indole moiety, and thereby promoting electrophilic substitution and stabilizing the carbocation intermediate. Other substituted tryptophans that were >50 % converted include those containing an electron-donating hydroxy group (6) or a methyl group (4), in which the latter has been shown to have an inductively electron-withdrawing and weakly mesomerically electron-donating effect on the indole moiety [38]. To examine the effect of the bulkiness of the substituents on the conversion, the van der Waals volume of the substituted tryptophans was calculated (Method S2) and used as an estimation of the bulkiness (Table S4). Generally, the observed trend (with 5-methyl-L-tryptophan as an exception) was that conversion was inversely related with the calculated volume of the substrate. This suggests that, besides electronic properties, steric constraints also play a role in the extent of substrate conversion by RePT.

Previously we established that RePT prenylates L-tryptophan at the *C*7- or *N*1-position, while phenolic substrates such as L-tyrosine, stilbenes, and other plant phenolics were primarily *O*-prenylated [25]. Here we found that RePT mainly prenylated the *C*7- or *N*1-position of various substituted L-tryptophans (Fig. 3). For 5-hydroxy-L-tryptophan (6), the only phenolic substrate tested in the current study, was mainly *C*-prenylated with only a minor amount of *O*-prenylation. Notably, only *C*5-halogenated tryptophans (8, 12, 15) showed a shift in regioselectivity from *C*7-prenylation towards *N*1-prenylation, which will be discussed in more detail in the section below.

Other DMATSs showed varying behavior in the conversion of *C*5-substituted tryptophans. For example, 7-DMATS$_{Afu}$ relatively poorly accepted 5-fluoro-L-tryptophan as a substrate when compared to *C*5 methylated, methoxylated, and hydroxylated tryptophan analogs [28]. In the case of DmaW (a 4-DMATS), *C*5-methyl substitution was found to disrupt polar interactions with key catalytic residues, making 5-methyl tryptophan a poorer substrate than the bulkier 5-methoxy tryptophan [39]. In contrast, for 7-DMATS$_{Neo}$, *C*5-methylated tryptophan was better accepted than its *C*5-methoxylated form, while its hydroxylated form was not accepted [18]. As RePT accepted 5-hydroxy- and 5-methyl-tryptophan much better than 5-methoxy tryptophan (Fig. 3), it deviates from DmaW and DMATS$_{Neo}$. Thereby, these observations show that the effect of substitution of tryptophan derivatives on their prenylation by DMATS is enzyme-specific.

3.5. Halogenation at various positions on the benzene moiety steers the regioselectivity of prenylation by RePT

In addition to studying the prenylation of *C*5-substituted tryptophans, we investigated, for the first time, the prenylation of a broad range of halogenated substrates by a fungal DMATS. We observed that RePT also catalyzed the prenylation of *C*4, *C*6, and *C*7 halogenated L-tryptophans (7, 9–11, 13, 14), with the fluorinated tryptophans showing a higher conversion than the corresponding chlorinated tryptophans (Fig. 3). In terms of product profile, RePT generated prenylated halogenated tryptophans with a varying ratio of *C*7- and *N*1-prenylated products.

Interestingly, both the conversion and regioselectivity strongly varied with the position of halogenation. Halogenation at *C*5 affected RePT activity more than halogenation at the other positions. As an example, 5-chloro-L-tryptophan was less converted compared to its 4-chloro and 6-chloro counterparts (Fig. 3). Notably, in terms of regioselectivity, *C*5-fluorination of 1 shifted the regioselectivity of RePT to *N*1-prenylation, whereas *C*4- and *C*6-fluorination (7 and 9) yielded the usual *C*7-prenylation. A slightly higher preference for *N*- than *C*-prenylation occurred in the case of 4-chloro and 5-chloro-L-tryptophan (11 and 12; Fig. 3). Moreover, *C*6-halogenation of 1 drove the reaction almost completely towards *C*-prenylation. By relative abundance, 95 % of 6-fluoro-L-tryptophan (9) was *C*7-prenylated and 97 % of 6-chloro-L-tryptophan (13) was *C*-prenylated (position unidentified), compared to 80 % *C*7-prenylation for 1 (Fig. 3, Table S3). Despite preferring *C*7-prenylation of 1, RePT was still able to prenylated *C*7-fluorinated (10) or *C*7-chlorinated (14) substrates. Nevertheless, on these substrates, the primary position of prenylation shifted to *N*1, while the exact prenylation position of the minor products could not be determined from MS^2 data. However, with 10, minor *C*-prenylation is speculated to most likely occur at *C*6 due to its adjacency to the originally preferred position. The shift in prenylation to a neighboring position is commonly observed in other DMATSs when their preferred site is substituted [17,20,40].

It is likely that for RePT, the regioselectivity shift is related to halogen-induced electron distribution changes across the indole moiety. It seems that *C*6-halogen substituents may act as *ortho/para* directors via their mesomeric electron-donating effect [38], enhancing the nucleophilicity of *C*7 over *N*1 and thereby facilitating *C*7-prenylation. Likewise, the shift in regioselectivity observed with *C*5-halogenated tryptophans may result from the reduced nucleophilicity of *C*7, a *meta* position [38], making the position less prone to electrophilic substitution and thereby increasing the likelihood of *N*1-prenylation.

While halogen-induced electronic effects on the indole moiety appear to strongly influence regioselectivity for several substrates, it should be noted that other factors have also been proposed to affect the regioselectivity of DMATSs, including substrate orientation relative to the prenyl moiety of a prenyl donor [22,35], substrate alignment with the proton-abstracting residue in the final reaction step [34,41], and steric constraints within the binding pocket [22]. For RePT, we hypothesize that these factors can overshadow the halogens' directing effect in certain substrates [35], based on the following observations: (i) 4-fluoro and 4-chloro substitution of L-tryptophan did not drive more prenylation towards *C*5 (*ortho*) or *C*7 (*para*); (ii) 7-fluoro and 7-chloro substitution did not drive more prenylation towards *C*6 (*ortho*) or *C*4 (*para*) but rather towards *N*1; and (iii) regardless of the substitution position, the prenylation by RePT occurred primarily on one side of the indole moiety (i.e., *C*6, *C*7, and *N*1). In accordance with this hypothesis, Liu and colleagues recently proposed that in the T102N variant of FgaPT2, the initial *C*6-prenylation site is guided by the relative nucleophilicity of the aromatic carbons, while the final *C*5-position of prenylation is determined largely by the proximity between the aromatic carbons and the proton-abstracting residue. By repositioning this residue to be closer to *C*5, they successfully shifted the regioselectivity of FgaPT2 from *C*4- to *C*5-prenylation of tryptophan [34]. This hints at the potential to fine-tune the regioselectivity of DMATSs by combining rational enzyme design and deliberate selection of substituted substrates.

3.6. Prenylation of indoles with different substituents on C3 of the pyrrole moiety

As indicated in the introduction, a large number of indole derivatives are known to be metabolites that play crucial roles as natural products or intermediates in biosynthetic pathways. Examples that were included in our study (Table S1) are: indole-3-carboxylic acid (16), a mediator in plant resistance mechanisms [42]; indole-3-acetic acid (17), an essential plant hormone [43]; indole-3-propionic acid (18), a neuroprotectant [44]; serotonin (20), a neurotransmitter and regulator of various biological processes [45]; brassinin (21) and camalexin (22), phytoalexins [46]; and tryptamine (19) and indole (23), which are (bio)synthetic precursors for numerous biologically active molecules [47]. All these indole derivatives share the same indole scaffold, but differ in their *C*3 substituents. The conversion and prenylation of these aromatic compounds by RePT was assessed (Fig. 4). Since a wide range of conversion

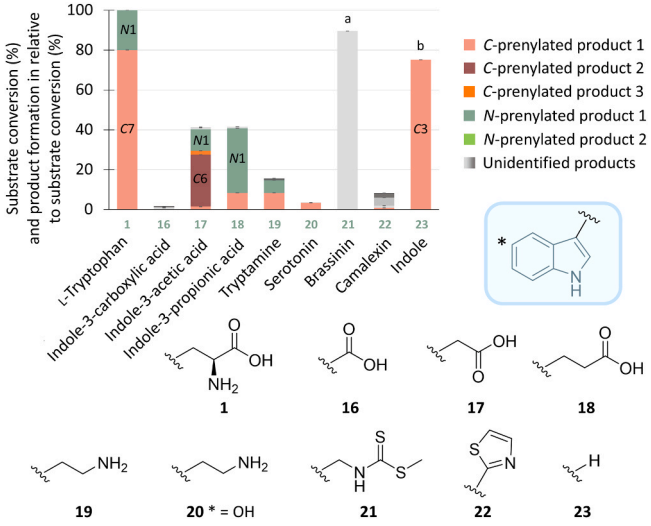

Fig. 4. Substrate conversion and product profile of prenylation of indole derivatives with varying *C*3-substituents by RePT. Selected prenylated products of which the chemical structures were confirmed by NMR analysis are labeled with their prenylation position (normal *C*6- or reverse *N*1-prenylation). The standard deviations indicated are the deviations for each product's formation relative to substrate conversion (%), while the standard deviations for substrate conversion are provided in Table S3. The asterisk indicates the site of the substitution by a hydroxyl group on substrate 20. [a] Conversion and product abundance of compound 21 could not be reliably identified, see explanation in Appendix B (Fig. S5). [b] A different product profile was observed upon modifying the reaction condition for upscaling of indole (23) prenylation (see Table S3 and Fig. S9).

(1.5–75.2 %; Fig. 4) was found, we discuss conversion of this set of substrates in more detail focusing on specific structural variations of their *C*3-substituents, such as absence of the α-amino group or the α-carboxyl group, or both.

Aromatic compounds lacking the α-amino group (17 and 18), were still converted by RePT, albeit to a reduced extent (around 40 %). For $DMATS1_{Ff}$, it has been shown that the substrate's α-amino group forms a hydrogen bond with the carbonyl groups of two amino acid residues (F81 and M82) [35]. Analogous residues in RePT would be F111 and M112, and hence, we hypothesized that interaction with these residues facilitates optimal substrate binding and prenylation, as observed in $DMATS1_{Ff}$ (Fig. S6). These two residues of $DMATS1_{Ff}$ are conserved beyond RePT in *O*-tyrosine-prenylating DMATSs (i.e., SirD, TyrPT, As-DMATS, Ri-DMATS, see Fig. S7A). Likewise, two residues were highlighted for the same function in FgaPT2 (*C*4-DMATS), but instead of F111 and M112, these analogous residues were I80 and L81 [22]. The absence of the α-amino group appears to influence not only the extent of conversion by RePT, but also the regioselectivity of prenylation. For 18, the prenylation primarily occurred as reverse *N*1-prenylation, while for 17 the main position of prenylation was normal *C*6, which differs from the *C*7 prenylation observed for 1.

Absence of the carboxyl group resulted in an even lower conversion than absence of the α-amino group, as illustrated by comparing 19 (16 %) and 20 (4 %) to 18 (42 %) (Table S3). Similar to the amino group, the substrate's carboxyl group was shown for $DMATS1_{Ff}$ to interact with two catalytic site residues via hydrogen bonds (Fig. S6) [35]. Their analogs in RePT, R290 and Y429, aligned with those from $DMATS1_{Ff}$ (R257 and Y389) and again, also seemed conserved within the characterized *O*-tyrosine-prenylating DMATSs (Fig. S7B). On another note, the presence of the α-carboxyl group too close to the pyrrole ring seems to hinder RePT's catalytic action substantially, as 16 was hardly prenylated by RePT. Although it has been suggested that hydrogen bonding via either the α-amino group or α-carboxyl group of the substrate is important for various DMATSs, the relative importance of one group over the other remains elusive [16,18,19,28].

Beyond hydrogen bonding via the α-amino group or α-carboxyl group, the indole ring also plays a role in binding, as seen with the high conversion of indole by RePT (23), a substrate lacking both groups. In the substrate screening, RePT was observed to only prenylated 23 at the *C*3 position (23a). Unlike other substrates, indole's NH is the sole hydrogen bond donor and potential substrate-binding site of 23. The absence of *C*7-prenylation amongst the confirmed products (23a, 23c, 23d), along with the formation of diverse *C*3-prenylated products, suggests that less extensive hydrogen bonding of 23 within the active site gives it higher orientational freedom compared to other substrates. It is also worth noting that *C*3 of indole is the most reactive site for electrophilic attack due to its high proton affinity [48], which may contribute to the observed *C*3-mono-prenylation (23a). Yet, when other reaction conditions were tested for the upscaled production of prenylated products, including the use of higher substrate to enzyme ratio and the addition of $CaCl_2$, RePT also catalyzed formation of three di-prenylated indoles (23b, 23c, 23d; Fig. 2 and Table S6). The increased yield of di-prenylated indoles likely resulted from the higher overall conversion observed in the upscaled production conditions (Fig. S8-9). Apparently, initially *C*3-mono-prenylated indole (23a), can act as substrate resulting in a second prenylation mainly at either *C*6 (23c) or *N*1 (23d) under the specified conditions.

The sulfur-containing compound brassinin (21) was well-converted, whereas camalexin (22) with its thiazole substituent was poorly converted. Although the extent of conversion of 21 could not be determined precisely due to its seemingly instable nature, the presence of prenylated products of 21 was observed (Fig. S5).

4. Conclusion

Our study demonstrates that RePT can catalyze prenylation of a wide variety of structurally diverse indole derivatives, enabling the production of *C*- and *N*-prenylated indole and tryptophan derivatives. Notably, we found that substituents such as halogens can be used to direct the prenylation position, allowing for selective control over prenylation at either the *C*7 or the *N*1 position through RePT's dual regioselectivity. Moreover, the high conversion of various fluorinated and chlorinated tryptophans by RePT opens up possibilities to create diverse (reactive) products that could serve as leads for novel pharmaceutical development or as intermediate building blocks for biocatalytic synthesis of biologically active compounds.

CRediT authorship contribution statement

van Berkel Willem J. H.: Writing – review & editing, Conceptualization. **Wouter J.C. de Bruijn:** Writing – review & editing, Supervision, Methodology, Conceptualization. **Mirjam A. Kabel:** Writing – review & editing, Supervision, Conceptualization. **Jean-Paul Vincken:** Writing – review & editing, Supervision. **Pimvisuth Chunkrua:** Writing – review & editing, Writing – original draft, Visualization, Methodology, Investigation, Formal analysis, Conceptualization.

Funding

This work was financially supported by Wageningen University and Anandamahidol Foundation (Thailand).

Declaration of Competing Interest

The authors have no conflict of interest.

Acknowledgments

The authors thank Jan Koek (Wageningen University) for insightful discussions on the reactivity of indoles; René Kuijpers and Margaret Bosveld (Wageningen University) for assistance with enzyme production; Janniek Ritsema (Wageningen University) for support with the NMR analysis; Mark Sanders (Wageningen University) for help with the UHPLC-ESI-Orbitrap-MS analysis; and Marina Ika Irianti (Wageningen University) for help with molecular descriptor calculations using MOE. Part of the presented results were obtained using an LTQ Velos Pro ion trap mass spectrometer, Orbitrap IQ-X mass spectrometer, and ÄKTA Pure 150 M chromatography system owned by WUR-Shared Research Facilities. Investment by WUR-Shared Research Facilities was made possible by the 'Regio Deal Foodvalley' of the province of Gelderland, The Netherlands. The MAGNEFY facility at Wageningen University (part of the Dutch national uNMR-NL facility) is gratefully acknowledged for the access to the NMR instruments.

Appendix A. Supporting information

Supplementary data associated with this article can be found in the online version at doi:10.1016/j.nbt.2025.09.002.

Data availability

Data will be made available on request.

References

[1] Klas KR, Kato H, Frisvad JC, Yu F, Newmister SA, Fraley AE, et al. Structural and stereochemical diversity in prenylated indole alkaloids containing the bicyclo [2.2.2]diazaoctane ring system from marine and terrestrial fungi. Nat Prod Rep 2018;35:532–58. https://doi.org/10.1039/c7np00042a.

[2] Cui C-B, Kakeya H, Okada G, Onose R, Osada H. Novel mammalian cell cycle inhibitors, tryprostatins A, b and other diketopiperazines produced by *Aspergillus fumigatus*. I. taxonomy, fermentation, isolation and biological properties. J Antibiot 1996;49:527–33. https://doi.org/10.7164/antibiotics.49.527.

[3] Jain HD, Zhang C, Zhou S, Zhou H, Ma J, Liu X, et al. Synthesis and structure-activity relationship studies on tryprostatin A, an inhibitor of breast cancer resistance protein. Bioorg Med Chem 2008;16:4626–51. https://doi.org/10.1016/j.bmc.2008.02.050.

[4] Kato H, Yoshida T, Tokue T, Nojiri Y, Hirota H, Ohta T, et al. Notoamides A-D: prenylated indole alkaloids isolated from a marine-derived fungus, *Aspergillus* sp. Angew Chem Int Ed 2007;46:2254–6. https://doi.org/10.1002/anie.200604381.

[5] Kartzinel R, Teychenne P, Gillespie MM, Perlow M, Gielen AC, Sadowsky DA, et al. Bromocriptine and levodopa (with or without carbidopa) in parkinsonism. Lancet 1976;308:272–5. https://doi.org/10.1016/S0140-6736(76)90728-5.

[6] Amant F, Spitz B, Timmerman D, Corremans A, Van Assche FA. Misoprostol compared with methylergometrine for the prevention of postpartum haemorrhage: a double-blind randomised trial. BJOG 1999;106:1066–70. https://doi.org/10.1111/j.1471-0528.1999.tb08115.x.

[7] Therien AG, Huber JL, Wilson KE, Beaulieu P, Caron A, Claveau D, et al. Broadening the spectrum of β-lactam antibiotics through inhibition of signal peptidase type I. Antimicrob Agents Chemother 2012;56:4662–70. https://doi.org/10.1128/AAC.00726-12.

[8] Perez-Bonilla M, Oves-Costales D, Gonzalez I, de la Cruz M, Martín J, Vicente F, et al. Krisynomycins, imipenem potentiators against methicillin-resistant *Staphylococcus Aureus*, produced by *Streptomyces canus*. J Nat Prod 2020;83:2597–606. https://doi.org/10.1021/acs.jnatprod.0c00294.

[9] Wang H, Yang Y, Abe I. Modifications of prenyl side chains in natural product biosynthesis. Angew Chem Int Ed 2024;63:e202415279. https://doi.org/10.1002/anie.202415279.

[10] de Bruijn WJC, Araya-Cloutier C, Bijlsma J, de Swart A, Sanders MG, de Waard P, et al. Antibacterial prenylated stilbenoids from peanut (*Arachis hypogaea*). Phytochem Lett 2018;28:13–8. https://doi.org/10.1016/j.phytol.2018.09.004.

[11] Araya-Cloutier C, Vincken J-P, van Ederen R, den Besten HMW, Gruppen H. Rapid membrane permeabilization of *Listeria Monocytogenes* and *Escherichia coli* induced by antibacterial prenylated phenolic compounds from legumes. Food Chem 2018;240:147–55. https://doi.org/10.1016/j.foodchem.2017.07.074.

[12] Kalli S, Araya-Cloutier C, Hageman J, Vincken J-P. Insights into the molecular properties underlying antibacterial activity of prenylated (iso)flavonoids against MRSA. Sci Rep 2021;11:14180. https://doi.org/10.1038/s41598-021-92964-9.

[13] Jeong A, Suazo KF, Wood WG, Distefano MD, Li L. Isoprenoids and protein prenylation: implications in the pathogenesis and therapeutic intervention of Alzheimer's disease. Crit Rev Biochem Mol Biol 2018;53:279–310. https://doi.org/10.1080/10409238.2018.1458070.

[14] Kelly SP, Shende VV, Flynn AR, Dan Q, Ye Y, Smith JL, et al. Data science-driven analysis of substrate-permissive diketopiperazine reverse prenyltransferase NotF: applications in protein engineering and cascade biocatalytic synthesis of (-)-eurotiumin a. J Am Chem Soc 2022;144:19326–36. https://doi.org/10.1021/jacs.2c06631.

[15] Fan A, Winkelblech J, Li SM. Impacts and perspectives of prenyltransferases of the DMATS superfamily for use in biotechnology. Appl Microbiol Biotechnol 2015;99:7399–415. https://doi.org/10.1007/s00253-015-6813-9.

[16] Steffan N, Unsöld IA, Li SM. Chemoenzymatic synthesis of prenylated indole derivatives by using a 4-dimethylallyltryptophan synthase from *Aspergillus fumigatus*. ChemBioChem 2007;8:1298–307. https://doi.org/10.1002/cbic.200700107.

[17] Takahashi S, Takagi H, Toyoda A, Uramoto M, Nogawa T, Ueki M, et al. Biochemical characterization of a novel indole prenyltransferase from *Streptomyces* sp. Sn-593. J Bacteriol 2010;192:2839–51. https://doi.org/10.1128/JB.01557-09.

[18] Miyamoto K, Ishikawa F, Nakamura S, Hayashi Y, Nakanishi I, Kakeya H. A 7-dimethylallyl tryptophan synthase from a fungal *Neosartorya* sp.: biochemical characterization and structural insight into the regioselective prenylation. Bioorg Med Chem 2014;22:2517–28. https://doi.org/10.1016/j.bmc.2014.02.031.

[19] Yu X., Liu Y., Xie X., Zheng X.D., Li S.M.Biochem Charact indole prenyltransferases Fill last gap prenylation Positions a 5dimethylallyl tryptophan synthase Aspergillus clavatus JBC28713711380 10.1074/jbc.M111.317982, 2012.

[20] Rudolf JD. Poulter cD. Tyrosine *o*-prenyltransferase sirD catalyzes *s*-, *c*-, and *n*-prenylations *on* tyrosine and tryptophan derivatives. ACS Chem Biol 2013;8:2707–14. https://doi.org/10.1021/cb400691z.

[21] Tudzynski P, Correia T, Keller U. Biotechnology and genetics of ergot alkaloids. Appl Microbiol Biotechnol 2001;57:593–605. https://doi.org/10.1007/s002530100801.

[22] Metzger U, Schall C, Zocher G, Unsöld I, Stec E, Li SM, et al. The structure of dimethylallyl tryptophan synthase reveals a common architecture of aromatic prenyltransferases in fungi and bacteria. Proc Natl Acad Sci USA 2009;106:14309–14. https://doi.org/10.1073/pnas.0904897106.

[23] Grundmann A, Li SM. Overproduction, purification and characterization of FtmPT1, a brevianamide f prenyltransferase from *Aspergillus fumigatus*. Microbiology 2005;151:2199–207. https://doi.org/10.1099/mic.0.27962-0.

[24] Ding Y, Wet JRD, Cavalcoli J, Li S, Greshock TJ, Miller KA, et al. Genome-based characterization of two prenylation steps in the assembly of the stephacidin and notoamide anticancer agents in a marine-derived *Aspergillus* sp. J Am Chem Soc 2010;132:12733–40. https://doi.org/10.1021/ja1049302.

[25] Chunkrua P, Leschonski KP, Gran-Scheuch AA, Vreeke GJC, Vincken J-P, Fraaije MW, et al. Prenylation of aromatic amino acids and plant phenolics by an aromatic prenyltransferase from *Rasamsonia emersonii*. Appl Microbiol Biotechnol 2024;108:421. https://doi.org/10.1007/s00253-024-13254-8.

[26] Faleye OS, Boya BR, Lee JH, Choi I, Lee J. Halogenated antimicrobial agents to combat drug-resistant pathogens. Pharm Rev 2024;76:90–141. https://doi.org/10.1124/pharmrev.123.000863.

[27] Adak S, Moore BS. Cryptic halogenation reactions in natural product biosynthesis. Nat Prod Rep 2021;38:1760–74. https://doi.org/10.1039/d1np00010a.

[28] Kremer A, Li SM. Potential of a 7-dimethylallyltryptophan synthase as a tool for production of prenylated indole derivatives. Appl Microbiol Biotechnol 2008;79:951–61. https://doi.org/10.1007/s00253-008-1505-3.

[29] Irianti MI, Malloci G, Ruggerone P, Lodinsky EV, Vincken J-P, Pos KM, et al. Indole phytochemical camalexin as a promising scaffold for AcrB efflux pump inhibitors against *Escherichia coli*. Biomed Pharm 2025;182:117779. https://doi.org/10.1016/j.biopha.2024.117779.

[30] Kremer A, Westrich L, Li SM. A 7-dimethylallyltryptophan synthase from *Aspergillus fumigatus*: overproduction, purification and biochemical characterization. Microbiology 2007;153:3409–16. https://doi.org/10.1099/mic.0.2007/009019-0.

[31] Schäfer T, Haun F, Gressler M, Spiteller P, Hoffmeister D. Parallel evolution *of* asco- and basidiomycete *o*-prenyltransferases. J Nat Prod 2024;87:576–82. https://doi.org/10.1021/acs.jnatprod.3c01120.

[32] Fan A, Chen H, Wu R, Xu H, Li SM. A new member of the DMATS superfamily from *Aspergillus niger* catalyzes prenylations of both tyrosine and tryptophan derivatives. Appl Microbiol Biotechnol 2014;98:10119–29. https://doi.org/10.1007/s00253-014-5872-7.

[33] Winkelblech J, Xie X, Li SM. Characterisation of 6-DMATS$_{Mo}$ from *Micromonospora olivasterospora* leading to identification of the divergence in enantioselectivity, regioselectivity and multiple prenylation of tryptophan prenyltransferases. Org Biomol Chem 2016;14:9883–95. https://doi.org/10.1039/c6ob01803c.

[34] Liu Y, Yao Y, Siddique K, Bai L, Liu G, Shi T. Understanding and engineering of C4 indole prenyltransferase FgaPT2 by theoretical study and mutation experiments. ACS Catal 2025;15:4921–33. https://doi.org/10.1021/acscatal.4c06489.

[35] Eaton SA, Ronnebaum TA, Roose BW, Christianson DW. Structural basis of substrate promiscuity and catalysis by the reverse prenyltransferase *n*-dimethylallyl-L-tryptophan synthase from *Fusa*rium fujikuroi. Biochemistry 2022;61:2025–35. https://doi.org/10.1021/acs.biochem.2c00350.

[36] Brown HC, Okamoto Y. Electrophilic substituent constants. J Am Chem Soc 1958;80:4979–87. https://doi.org/10.1021/ja01551a055.

[37] Luk LYP, Tanner ME. Mechanism of dimethylallyltryptophan synthase: evidence for a dimethylallyl cation intermediate in an aromatic prenyltransferase reaction. J Am Chem Soc 2009;131:13932–3. https://doi.org/10.1021/ja906485u.

[38] Otero N, Mandado M, Mosquera RA. Nucleophilicity of indole derivatives: activating and deactivating effects based on proton affinities and electron density properties. J Phys Chem A 2007;111:5557–62. https://doi.org/10.1021/jp0708953.

[39] Eggbauer B, Schrittwieser JH, Kerschbaumer B, Macheroux P, Kroutil W. Regioselective biocatalytic *c*4-prenylation of unprotected tryptophan derivatives. ChemBioChem 2022;23:e202200311. https://doi.org/10.1002/cbic.202200311.

[40] Rudolf JD, Wang H, Poulter CD. Multisite prenylation of 4-substituted tryptophans by dimethylallyltryptophan synthase. J Am Chem Soc 2013;135:1895–902. https://doi.org/10.1021/ja310734n.

[41] Ostertag E, Zheng L, Broger K, Stehle T, Li SM, Zocher G. Reprogramming substrate and catalytic promiscuity of tryptophan prenyltransferases. J Mol Biol 2021:433. https://doi.org/10.1016/j.jmb.2020.11.025.

[42] Gamir J, Pastor V, Sánchez-Bel P, Agut B, Mateu D, García-Andrade J, et al. Starch degradation, abscisic acid and vesicular trafficking are important elements in callose priming by indole-3-carboxylic acid in response to plectosphaerella cucumerina infection. Plant J 2018;96:518–31. https://doi.org/10.1111/tpj.14045.

[43] Zhao Y. Auxin biosynthesis and its role in plant development. Annu Rev Plant Biol 2010;61:49–64. https://doi.org/10.1146/annurev-arplant-042809-112308.

[44] Kim CS, Jung S, Hwang GS, Shin DM. Gut microbiota indole-3-propionic acid mediates neuroprotective effect of probiotic consumption in healthy elderly: a randomized, double-blind, placebo-controlled, multicenter trial and in vitro study. Clin Nutr 2023;42:1025–33. https://doi.org/10.1016/j.clnu.2023.04.001.

[45] Berger M, Gray JA, Roth BL. The expanded biology of serotonin. Annu Rev Med 2009;60:355–66. https://doi.org/10.1146/annurev.med.60.042307.110802.

[46] Sellam A, Iacomi-Vasilescu B, Hudhomme P, Simoneau P. *In vitro* antifungal activity of brassinin, camalexin and two isothiocyanates against the crucifer pathogens *Alternaria brassicicola* and *Alternaria brassicae*. Plant Pathol 2007;56:296–301. https://doi.org/10.1111/j.1365-3059.2006.01497.x.

[47] McDonald AD, Perkins LJ, Buller AR. Facile *In vitro* biocatalytic production of diverse tryptamines. ChemBioChem 2019;20:1939–44. https://doi.org/10.1002/cbic.201900069.

[48] Otero N, González Moa MJ, Mandado M, Mosquera RA. QTAIM study of the protonation of indole. Chem Phys Lett 2006;428:249–54. https://doi.org/10.1016/j.cplett.2006.07.059.